ELSEVIER

Carbohydrate Polymers 47 (2002) 313–321

Carbohydrate Polymers

www.elsevier.com/locate/carbpol

Description of the thermodynamic incompatibility of the guar–dextran aqueous two-phase system by light scattering

F. Simonet, C. Garnier, J.-L. Doublier*

Unité de Physico-Chimie des Macromolécules, INRA, BP 71627, 44316 Nantes cedex 3, France

Received 22 September 2000; revised 15 December 2000; accepted 18 January 2001

Abstract

The phase diagram of the guar–dextran aqueous two-phase system has been described on the basis of static light scattering measurements in the dilute regime. By determining the molar weight and second virial coefficient from the two single polymers and the second virial cross coefficient from mixtures at constant guar/dextran ratio (either 17/83 or 28/72), the thermodynamic models based on the virial expansion or the Flory–Huggins theory were successfully applied. The second virial coefficient of guar was difficult to estimate with enough accuracy by light scattering and therefore was obtained by adjustment using a simple criterion stating that the calculated spinodal passes through the experimental critical point. The obtained value was within the confidence interval given by light scattering. Virial expansion and Flory–Huggins approaches yielded quite similar theoretical phase diagrams that satisfactorily fitted the experimental one. The slight discrepancies observed on the position of binodals and critical points has been attributed to the polydispersity of guar or the difficulty in extrapolating from the dilute regime to the semidilute one. The slope of the tie-lines was predicted with a good accuracy, especially with the virial expansion model. The fact that both approaches gave such similar results is probably related to the fact that the expressions of chemical potentials are equivalent if the polymer concentrations are low enough. In this particular case, both models are based on excluded volume interactions and equally describe the phase behavior of the guar–dextran aqueous system.

Keywords: Guar gum; Dextran; Static light scattering; Phase diagram; Virial expansion model; Flory–Huggins theory

1. Introduction

Polysaccharides are widely used as thickeners or gelling agents in the food industry, especially in mixtures, either with other polysaccharides or with proteins. When dealing with biopolymer mixtures, thermodynamic incompatibility is a general phenomenon (Piculell, Bergfeldt & Nilsson, 1995; Tolstoguzov, 1998), which plays a key role in the physico-chemical properties of the medium. Phase diagrams of ternary mixtures containing two polysaccharides in aqueous solution have been first described for the methylcellulose–dextran system that may be used for the bioseparation of particles (Albertsson, 1962). More recently, the phase behavior of several polysaccharide–polysaccharide aqueous systems, i.e. dextran–amylose (Kalichevsky, Orford & Ring, 1986), amylose–amylopectin (Kalichevsky & Ring, 1987), dextran–agarose (Medin & Janson, 1993), locust bean gum–dextran (Garnier, Schorsch & Doublier, 1995), pectin–pectin (McDougall, Rigby & Ring, 1997), guar–amylopectin (Closs, Conde-Petit, Roberts, Tolstoguzov & Escher, 1999), and guar–dextran (Garnier, Bouchet, Gallant & Doublier, 1999; Simonet, Garnier & Doublier, 2000) has been described.

Other studies have treated this phenomenon in a theoretical way in order to establish general rules or model preexisting experimental phase diagrams. Most of these studies dealt with the polyethyleneoxide (PEO)–dextran aqueous system, which is commonly used for bioseparation and extensively described in the literature (Albertsson, 1986; Zaslavsky, 1995). Two different theoretical approaches were generally used. The first one, originally developed by Edmond and Ogston (1968), is essentially formal and based on the truncated virial expansion of chemical potentials. It has been used for the PEO–dextran aqueous system in a predictive way by Haynes, Benitez, Blanch and Prausnitz (1989), and improved by taking into account the effect of polydispersity (Cabezas, Evans & Szlag, 1989). The second one is based on the Flory–Huggins theory extended to ternary polymer–polymer–solvent systems by Scott (1949) and Tompa (1949). This approach has been applied to the computation of phase diagrams by Hsu and Prausnitz (1974), and more recently for aqueous systems containing

* Corresponding author. Tel.: +33-2-40-67-50-55; fax: +33-2-40-67-50-43.
E-mail address: doublier@nantes.inra.fr (J.-L. Doublier).

0144-8617/02/$ - see front matter
PII: S0144-8617(01)00176-X

polyelectrolytes (Piculell et al., 1995) or polysaccharides (Clark, 2000) on the basis of experimental results taken from the literature. Some improvements were made, considering the polydispersity of the polymer species (Vinches, Parker & Reed, 1997) and the concentration and temperature dependence of the interaction parameters (Koningsveld & Staverman, 1968; Mumby & Sher, 1994).

Besides these two approaches, other models featuring parameters that are difficult to obtain experimentally have been developed to describe the phase behavior of the PEO–dextran aqueous system. The UNIQUAC model of Kang and Sandler (1987) considers the structure of the macromolecules and the polydispersity (Kang & Sandler, 1988) but needs some adjustable parameters. A model based on statistical geometry and excluded volume considerations has been described by Guan, Lilley and Treffry (1993). This relatively concise model needs only one adjustable parameter to satisfactorily describe the coexistence curve. The semiempirical model of Großmann, Tintinger, Zhu and Maurer (1995) can take into account the influence of polymer molar weight and temperature but needs a lot of adjustable parameters. The modified NRTL (non-random two-liquid) model developed by Wu, Zhu, Lin and Mei (1996) provides a good description of the phase diagrams (da Silva & Meirelles, 2000) but needs many adjustable parameters as well.

In the present work, the guar–dextran mixture has been chosen as a model of polysaccharide–polysaccharide segregative aqueous two-phase system (Garnier et al., 1999; Simonet et al., 2000). The initial objective was to describe the guar–dextran phase diagram on the basis of static light scattering data. Two thermodynamic approaches have been used, based either on the virial expansion or the Flory–Huggins theory. All the parameters of these models may be experimentally determined by a study of the single polymers and mixtures in the dilute regime, yielding molar weights and second virial coefficients. The accuracy of these predictive approaches will be discussed in terms of description of the experimental phase diagram regarding the precision of the light scattering measurements.

2. Materials and methods

2.1. Materials

Guar is a galactomannan, i.e. a neutral polysaccharide consisting of a β-(1-4)-mannan-backbone substituted by α-(1-6)-linked galactosyl units (mannose/galactose ratio ~1.6–1.8) extracted from leguminous seeds. In aqueous solution, guar acts as a random-coil polymer (Doublier & Launay, 1981; Robinson, Ross-Murphy & Morris, 1982) and exhibits thickening properties that are widely used in the food industry. The purified sample used in the present work was provided by SKW Biosystems (France). Its intrinsic viscosity in water at 25°C is about 12.9 dl g^{-1}, which leads to a weight-average molar weight of $\sim 1.9 \times 10^6$ g mol^{-1} according to the Mark–Houwink relationship established by Robinson et al. (1982) from static light scattering data.

Dextran is a microbial polysaccharide composed of α-(1–6)-linked glucose units. In aqueous solution, dextran behaves like a random coil (Tvaroska, Perez & Marchessault, 1978). It is a highly flexible and slightly branched polymer, featuring a high solubility and a low viscosity with regard to guar. The sample of dextran T500 was provided by Pharmacia LKB Biotechnology AB (Sweden). Its intrinsic viscosity is about 0.51 dl g^{-1} in water at 25°C and its weight average molar weight is $\sim 5.2 \times 10^5$ g mol^{-1} with a polydispersity index $I \sim 2.2$, as determined by the supplier from low-angle light scattering.

2.2. Methods

The preparation of guar and dextran stock solutions as well as the determination of the guar–dextran phase diagram have been described in a previous paper (Simonet et al., 2000). Nevertheless, we improved the determination of the tie-lines and the guar-rich part of the binodal by centrifugating for 1 h at 20,000g instead of 3 h at 2600g, to ensure that the thermodynamic equilibrium was reached, with regard to the high viscosity of the medium.

The Rayleigh ratio R_θ was measured at $\lambda = 514.5$ nm using a Brookhaven Instruments Corporation goniometer over the range of scattering angles $\theta = 28$–$130°$. The temperature was set at 25°C and the instrument was calibrated with dust-free toluene ($R_{90°} = 3.3 \times 10^{-5}$ cm^{-1}). The refractive index increments of both polysaccharides were determined at 25°C using a Chromatix Kmx-16 laser differential refractometer at $\lambda = 633$ nm. The values $dn/dc \sim 0.151$ cm^3 g^{-1} and 0.155 cm^3 g^{-1} were obtained for dextran and guar, respectively. Considering the values found in the literature at different wavelengths ranging from 436 to 633 nm (Antonov, Lefebvre & Doublier, 1999; Arond & Frank, 1954; Burchard & Pfannemüller, 1969; Doublier, 1975; Rathbone, Haynes, Blanch & Prausnitz, 1990; Robinson et al., 1982; Senti et al., 1955), $dn/dc \sim 0.151$ $cm^3.g^{-1}$ was kept throughout for both polysaccharides. Prior to the light scattering measurements, the stock solutions were slowly filtered through membranes (surfactant free cellulose acetate, pore size 0.45 μm) and the concentrations were checked with a differential refractometer to ensure that they were not affected by the filtration process. All the solutions were in the dilute regime, i.e. below the overlap concentration c^* defined here as the inverse of the intrinsic viscosity. The concentration range was 0.1–0.3% w/w for dextran ($c^* \sim 2.0$% w/w) and 10^{-3}–10^{-2}% w/w for guar ($c^* \sim 8 \times 10^{-2}$% w/w). For the mixtures, measurements were performed at constant guar/dextran ratio, either 17/83 or 28/72, over one decade of concentrations far below c^* for both polysaccharides. In every Zimm representation, the constant angle curves

were adjusted with linear fits and the constant concentration curves with second order polynomials. The extrapolation to $\theta = 0$ led to the weight-average molar weight M_w and the second virial coefficient A_2, while the extrapolation to $c = 0$ gave M_w and the radius of gyration R_G. In the particular case of mixtures, the total polymer concentration had to be considered and these extrapolations yielded an "apparent" molar weight M_w^{app} and an "apparent" second virial coefficient A_{23}^{app}. As both refractive index increments were equal, M_w^{app} and A_{23}^{app} were related to the parameters of individual components and the second virial cross coefficient (Kratochvíl, Vorlícek, Straková & Tuzar, 1975) according to the following equations:

$$M_w^{app} = w_2 M_{w2} + w_3 M_{w3} \quad (1)$$

$$A_{23}^{app} = (M_{w2}^2 w_2^2 A_{22} + 2M_{w2}M_{w3}w_2 w_3 A_{23} + M_{w3}^2 w_3^2 A_{33})/(M_{w2}w_2 + M_{w3}w_3)^2 \quad (2)$$

wherein the subscripts 2 and 3 refer to the two solute components, M_{wi} is the weight average molar weight of polymer i, w_i the weight fraction of polymer i, and A_{ii} the second virial coefficient relative to the polymer i. A_{23} is the second virial cross coefficient accounting for interactions between polymer 2 and polymer 3. Therefore, the knowledge of A_{22}, A_{33}, M_{w2}, and M_{w3} from single polymer solutions, and A_{23}^{app} from a mixture in proportion w_2/w_3 yielded the second virial cross coefficient A_{23} using Eq. (2).

3. Theoretical framework

3.1. Model based on the virial expansion

The semiempirical thermodynamic approach of Edmond and Ogston (1968) was developed for dilute ternary systems containing two monodisperse neutral polymers in aqueous solution. The chemical potential of each species, i.e. solvent 1, polymer 2, and polymer 3 is expressed as a virial expansion truncated after the second term, three-body and higher order interactions being neglected:

$$\mu_1 = \mu_1^0 - (RTM_1/1000)(m_2 + m_3 + (a_{22}/2)m_2^2 + (a_{33}/2)m_3^2 + a_{23}m_2m_3) \quad (3a)$$

$$\mu_2 = \mu_2^0 + RT(\ln m_2 + a_{22}m_2 + a_{23}m_3) \quad (3b)$$

$$\mu_3 = \mu_3^0 + RT(\ln m_3 + a_{33}m_3 + a_{23}m_2) \quad (3c)$$

where m_i is the molality (mol kg^{-1}) of polymer i, a_{ii} the second virial coefficient of polymer i in molal units (kg mol^{-1}), a_{23} the second virial cross coefficient in molal units (kg mol^{-1}), μ_i^0 the standard state chemical potential of component i, M_1 the molar weight of solvent, and R and T are, respectively, the gas constant and absolute temperature.

The interaction parameters a_{22}, a_{33}, and a_{23} are directly related to the usual second virial coefficients according to:

$$a_{22} = 2M_{w2}^2 A_{22}/1000 \quad (4a)$$

$$a_{33} = 2M_{w3}^2 A_{33}/1000 \quad (4b)$$

$$a_{23} = 2M_{w2}M_{w3}A_{23}/1000 \quad (4c)$$

where 1000 represents the partial specific volume of water (cm^3 kg^{-1}).

The spinodal curve (Prigogine & Defay, 1954) representing the borderline between metastability and absolute instability is given by a hyperbola equation

$$(1/m_2 + a_{22})(1/m_3 + a_{33}) - a_{23}^2 = 0 \quad (5)$$

and the coordinates of the critical point are extracted from the following equations:

$$1/m_2^{crit} + a_{22} - a_{23}(m_3^{crit}/m_2^{crit})^{2/3} = 0 \quad (6a)$$

$$1/m_3^{crit} + a_{33} - a_{23}(m_2^{crit}/m_3^{crit})^{2/3} = 0 \quad (6b)$$

The binodal and the tie-lines are obtained by solving the equality of the chemical potentials of each species between both phases in equilibrium, designated by the superscripts $'$ and $''$:

$$\mu_1' = \mu_1'' \quad (7a)$$

$$\mu_2' = \mu_2'' \quad (7b)$$

$$\mu_3' = \mu_3'' \quad (7c)$$

By arbitrarily choosing the molality of one polymer in one phase, these latter conditions lead to a system of three nonlinear equations with three unknowns. Each resolution of this system yields two points of the binodal linked by a tie-line.

3.2. Model based on the Flory–Huggins theory

The Flory–Huggins theory (Flory, 1942, 1953; Huggins, 1942) considers a lattice model describing a semidilute solution of a flexible and monodisperse polymer where only short range interactions do occur. It has been extended to ternary systems containing two polymers in one solvent by Scott (1949) and Tompa (1949) and the application of this approach to aqueous systems containing polysaccharides has been recently discussed in detail by Clark (2000). The expressions of the chemical potentials for solvent 1, polymer 2, and polymer 3 are given by:

$$\mu_1 = \mu_1^0 + RT[\ln \phi_1 + (1 - 1/x_2)\phi_2 + (1 - 1/x_3)\phi_3 + \phi_2\phi_3(\chi_{12} + \chi_{13} - \chi_{23}) + \chi_{12}\phi_2^2 + \chi_{13}\phi_3^2] \quad (8a)$$

$$\mu_2 = \mu_2^0 + RT[\ln \phi_2 + (1 - x_2/x_3)\phi_3 + (1 - x_2)\phi_1 + x_2(\chi_{23}\phi_3^2 + \chi_{12}\phi_1^2 + \phi_1\phi_3(\chi_{12} + \chi_{23} - \chi_{13}))] \quad (8b)$$

$$\mu_3 = \mu_3^0 + RT[\ln \phi_3 + (1 - x_3/x_2)\phi_2 + (1 - x_3)\phi_1 + x_3(\chi_{23}\phi_2^2 + \chi_{13}\phi_1^2 + \phi_1\phi_2(\chi_{13} + \chi_{23} - \chi_{12}))] \quad (8c)$$

wherein ϕ_i is the volume fraction of component i, x_i the ratio of polymer i to solvent molar volumes, χ_{ij} the Flory–Huggins interaction parameter between species i and j, and the other symbols have the meanings already described.

The parameter x_i is defined as follows:

$$x_i = M_i v_i / M_1 v_1 \quad (9)$$

where M_i is the molar weight of polymer i, v_i the partial specific volume of polymer i, and M_1 and v_1 are the same parameters referring to the solvent.

By extrapolating toward the dilute regime, the Flory–Huggins interaction parameters can be calculated from the second virial coefficients with use of the following expressions (Flory, 1953):

$$\chi_{12} = 0.5 - v_1 M_1 A_{22}/v_2^2 \quad (10a)$$

$$\chi_{13} = 0.5 - v_1 M_1 A_{33}/v_3^2 \quad (10b)$$

$$\chi_{23} = 2v_1 M_1 A_{23}/v_2 v_3 - 1 + \chi_{12} + \chi_{13} \quad (10c)$$

The binodal and the tie-lines are obtained by combining the chemical potential expressions (8) with Eqs. (7). The volume fraction of one component is arbitrarily set and two material balances for the two phases are added, which yield a system of three non-linear equations with three unknowns as for the previous model. Each solution provides a couple of points in equilibrium.

4. Results and discussion

4.1. Static light scattering

Throughout the following development, indexes 2 and 3 will refer to dextran and guar, respectively. The Zimm plot for dextran in water is represented in Fig. 1. The extrapolation to zero angle yields the weight average molar weight $M_{w2} \sim 5.67 \times 10^5$ g mol^{-1} and the second virial coefficient $A_{22} \sim 1.63 \times 10^{-4}$ cm^3 mol g^{-2}. The extrapolation to zero concentration gives a similar value for the molar weight $M_{w2} \sim 5.67 \times 10^5$ g mol^{-1} and the radius of gyration $R_{G2} \sim 45.0$ nm. The molecular weight value is slightly higher than the one given by the supplier, but the above values are generally consistent with light scattering results reported in the literature for dextran T500 (Desbrières, Borsali, Rinaudo & Milas, 1993; Haynes et al., 1989; Haynes, Benitez, Blanch & Prausnitz, 1993; King, Blanch & Prausnitz, 1988; Wu, 1993). The slight downward curvature of the constant concentration curves on the whole range of angles may be related to the polydispersity of the dextran sample, rather than the stiffness of polymer chains since dextran molecules are highly flexible (Kratochvíl, 1972).

The Zimm plot for guar in water is shown in Fig. 2. Both

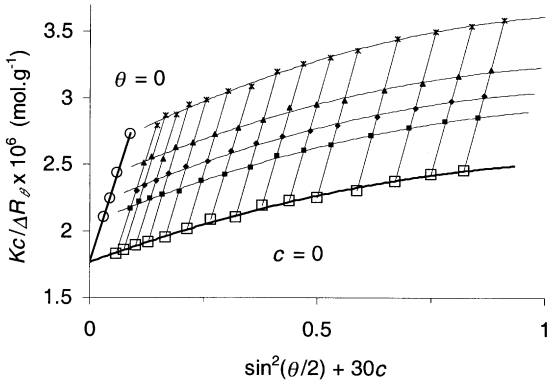

Fig. 1. Zimm plot for dextran in water at 25°C. The concentrations of the scattering solutions are 0.10 (■), 0.15 (◆), 0.20 (▲), and 0.30% w/w (×). Symbols (○) and (□) refer to the zero angle ($R^2 \sim 0.997$) and zero concentration ($R^2 \sim 0.996$) extrapolations, respectively.

extrapolations, to zero angle and zero concentration, yield the same weight-average molar weight $M_{w3} \sim 2.17 \times 10^6$ g mol^{-1}. On the other hand, the second virial coefficient has a relatively high uncertainty since the correlation coefficient of the zero angle extrapolation is low ($R^2 \sim 0.680$). This effect may be due to the presence of supramolecular assemblies that generate fluctuations in the scattered intensity (Robinson et al., 1982). As the concentration range is low (10^{-3}–10^{-2}% w/w), the slope of the zero angle linear fit is low as well and hence very sensitive to data dispersion. Four series of measurements, made with the same guar sample, yielded second virial coefficient values within the interval 3×10^{-4}–6×10^{-4} cm^3 mol g^{-2}, so that the value given in the present example ($A_{33} \sim 4.85 \times 10^{-4}$ cm^3 mol g^{-2}) must be considered as indicative. The extrapolation to zero concentration leads to the value $R_{G3} \sim 146$ nm for the radius of gyration. The overall values obtained in the present work for guar are generally consistent with the results in the literature (Antonov et al., 1999; Doublier, 1975). The weight average molar weight $M_{w3} \sim$

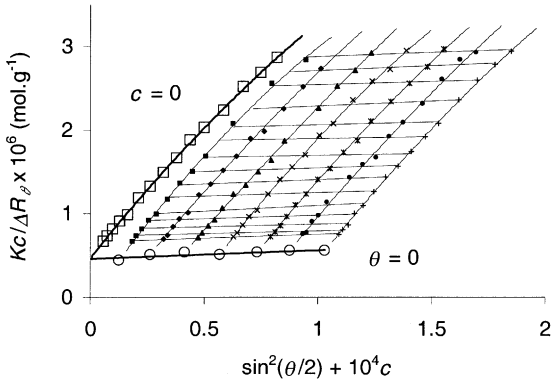

Fig. 2. Zimm plot for guar in water at 25°C. The concentrations of the scattering solutions are 0.0013 (■), 0.0026 (◆), 0.0041 (▲), 0.0057 (×), 0.0073 (∗), 0.0088 (●), and 0.010% w/w (+). Symbols (○) and (□) refer to the zero angle ($R^2 \sim 0.680$) and zero concentration ($R^2 \sim 0.999$) extrapolations, respectively.

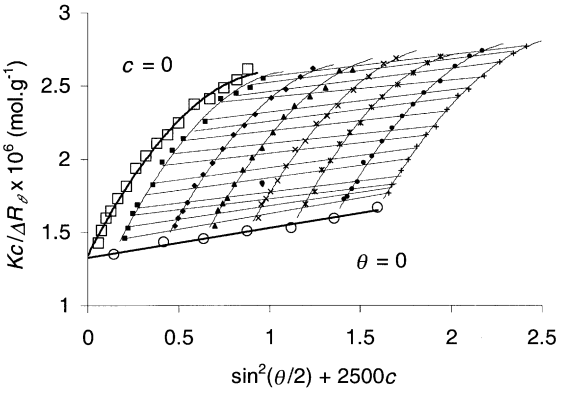

Fig. 3. Zimm plot for the guar/dextran mixture in proportion 17/83 in water at 25°C. The total concentrations of the scattering solutions are 0.0058 (■), 0.017 (◆), 0.025 (▲), 0.035 (×), 0.045 (*), 0.054 (●), and 0.064% w/w (+). Symbols (○) and (□) refer to the zero angle ($R^2 \sim 0.979$) and zero concentration ($R^2 \sim 0.997$) extrapolations, respectively.

2.17×10^6 g mol^{-1} that will be kept throughout is slightly higher than the value predicted by the Mark–Houwink relationship of Robinson et al. (1982), i.e. $M_{w3} \sim 1.85 \times 10^6$ g mol^{-1}, probably because it is obtained with second-order polynomial fits for the constant concentration curves. In fact, this procedure usually leads to higher values for the molar weight than the one using linear fits that actually yields $M_{w3} \sim 1.89 \times 10^6$ g mol^{-1}.

The Zimm plots for guar/dextran mixtures in proportions 17/83 and 28/72 are represented in Figs. 3 and 4, respectively. Both diagrams are curved, especially at high angle, which may be related to the bimodal size distribution of the scattering molecules (Kratochvíl, 1972). The "apparent" weight-average molar weight, respectively, $M_{wapp} \sim 7.54 \times 10^5$ g mol^{-1} and 9.23×10^5 g mol^{-1} for the two ratios, are close to the values calculated with Eq. (1) from single polymers data, i.e. $M_w^{app} \sim 8.35 \times 10^5$ g mol^{-1} and 1.01×10^6 g mol^{-1}. The "apparent" second virial coefficients

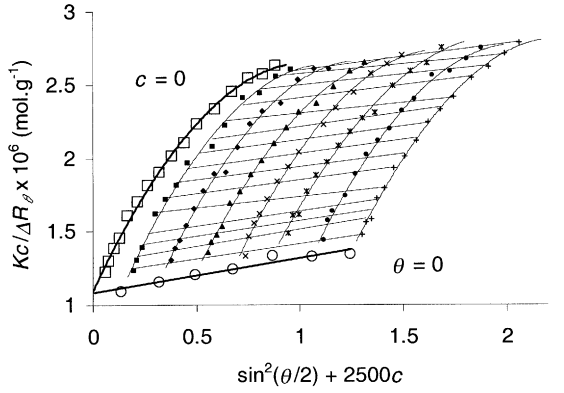

Fig. 4. Zimm plot for the guar/dextran mixture in proportion 28/72 in water at 25°C. The total concentrations of the scattering solutions are 0.0055 (■), 0.013 (◆), 0.020 (▲), 0.027 (×), 0.035 (*), 0.042 (●), and 0.050% w/w (+). Symbols (○) and (□) refer to the zero angle ($R^2 \sim 0.938$) and zero concentration ($R^2 \sim 0.997$) extrapolations, respectively.

measured from the slopes of the linear extrapolations to zero angle are $A_{23}^{app} \sim 2.53 \times 10^{-4}$ cm^3 mol g^{-2} and 2.93×10^{-4} cm^3 mol g^{-2} for the ratios 17/83 and 28/72, respectively. These values are determined with a much better accuracy ($R^2 \sim 0.979$ and 0.938, respectively) than for guar alone, probably because the scattered intensity of mixtures is less sensitive to the presence of guar aggregates.

4.2. Prediction of the guar–dextran phase diagram

The previously described theories do not take polydispersity into account. The values taken from light scattering experiments, i.e. weight-average molar weights and z-average second virial coefficient, were kept throughout since no information was available on number-average molar weights and weight-average second virial coefficients. The second virial coefficient A_{33} of guar that cannot be precisely measured by light scattering, has been adjusted according to the following criterion: for each guar/dextran ratio, the value of A_{33} can be determined in a way that the calculated spinodal curve, based on the virial expansion model, passes through the experimental critical point. Applying this, Eq. (5) leads to a second order polynomial in A_{33}, from which the value of the second virial coefficient of guar can be obtained unambiguously. Using this rather simple condition, no consideration of the experimental binodal or slope of the tie-lines is taken into account. For the guar/dextran ratios 17/83 and 28/72, the criterion yields $A_{33} \sim 3.25 \times 10^{-4}$ cm^3 mol g^{-2} and 3.50×10^{-4} cm^3 mol g^{-2}, respectively. These two values are relatively close with regard to the experimental error on the light scattering measurement of the second virial coefficient of guar. Moreover, they belong to the interval 3×10^{-4}–6×10^{-4} cm^3 mol g^{-2} that was experimentally estimated. The second virial cross coefficients corresponding to the aforementioned values of A_{33} and calculated with Eq. (2) are $A_{23} \sim 2.84 \times 10^{-4}$ cm^3 mol g^{-2} and 2.94×10^{-4} cm^3 mol g^{-2} for the ratios 17/83 and 28/72, respectively. As can be seen from Eq. (2), other guar/dextran ratios featuring higher amounts of guar are not suited for the determination of A_{23} because the term relative to guar then becomes very high compared to the other terms. Since the major source of error comes from that term, the 28/72 guar/dextran ratio appeared to be a reasonable upper limit. Molecular weights and second virial coefficients that will be used all through the following computations are summarized in Table 1. For both thermodynamic approaches, the resolution of Eqs. (7a)–(7c) can be performed with a numerical method like the Newton's method. To find a solution to an equation $f(x) = 0$, this iterative method starts at x_0 chosen by the user. Then it uses knowledge of the derivative f' to take a sequence of steps toward a solution. Each point x_n is deduced from the previous point x_{n-1} by the formula $x_n = x_{n-1} - f(x_{n-1})/f'(x_{n-1})$.

The calculated spinodal, binodal, and tie-lines, on the basis of a virial expansion for the two guar/dextran ratios, are shown in Fig. 5 and compared to the experimental phase diagram. Both ratios yield the same spinodal curve, which is

Table 1
Molar weights and second virial coefficients used for the computation of the guar/dextran phase diagram. Two guar/dextran ratios are considered. All the parameters are measured by light scattering, except * adjusted using the coincidence between the calculated spinodal and the experimental critical point (see text)

	Guar/dextran 17/83		Guar/dextran 28/72
$M_w^{dextran}$ (g mol^{-1})		5.67×10^5	
M_w^{guar} (g mol^{-1})		2.17×10^6	
$A_{22}^{dextran}$ (cm^3 mol g^{-2})		1.63×10^{-4}	
A_{33}^{guar} (cm^3 mol g^{-2})	3.25×10^{-4}*		3.50×10^{-4}*
A_{23}^{app} (cm^3 mol g^{-2})	2.53×10^{-4}		2.93×10^{-4}
A_{23} (cm^3 mol g^{-2})	2.84×10^{-4}*		2.94×10^{-4}*

located inside the experimental biphasic area, in agreement with the theory. As can be seen from Eq. (5), this curve is actually a hyperbola featuring two asymptotes parallel to the axis (0.13% w/w guar and 1.04% w/w dextran). The calculated binodal curve is practically the same for both guar/dextran ratios. It is relatively close to the experimental curve, especially at moderate guar concentrations, i.e. below 1% w/w, where the distance between both curves is less than 0.1% w/w. However, the experimental curve is slightly closer to the dextran axis in this area. This might be related to the polydispersity of guar since galactomannan samples are generally known to feature high indexes of polydispersity (Doublier, 1975; Sabater de Sabates, 1979). Such effects of polydispersity have been reported by Kang and Sandler (1988) and Shirataki and Kamide (1993) in theoretical studies on the phase behavior of quasi-ternary systems. Both studies conclude that as the broadness of the molar weight distribution of one polymer increases, the binodal curve shifts toward the other polymer axis and the biphasic region is enlarged. The neglected three-body and higher order interactions may also contribute to this slight discrepancy, as reported by Haynes et al. (1989). In fact, the present model extrapolates the results obtained in the dilute regime to the semidilute one while the virial expansion should be extended to the third or higher order term. The experimental and calculated tie-lines display a constant slope on the overall phase diagram. All the values, i.e. ~0.74 for the experimental and 0.75 (respectively, 0.73) for the calculated tie-lines with the 17/83 (respectively, 28/72) guar/dextran ratio are very close as can be seen in Fig. 5, pointing out that the partition of water between both phases is predicted with a very good accuracy. The calculated critical point corresponds to a mixture containing about 1.57% w/w dextran and 0.53% w/w guar for both ratios. These coordinates are also close to the experimental values, which are 1.66% w/w dextran and 0.47% w/w guar.

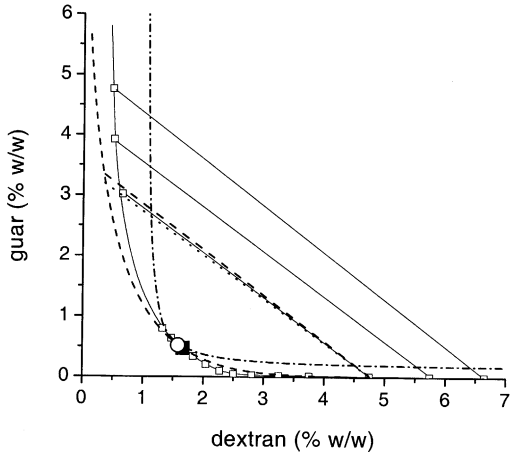

Fig. 5. Calculated binodal and tie-lines for the guar/dextran system using the virial expansion and the light scattering data of the 17/83 mixture (- - -). The 28/72 mixture yields the same binodal but slightly different tie-lines (···). The calculated spinodal for both ratios is also represented (-·-·-). The experimental binodal and tie-lines are represented with solid lines and symbols (—□—). Open symbol (○) refers to the calculated critical point and (■) represents the experimental critical point.

Before describing the phase diagram with the second model, based on the Flory–Huggins theory, it would be interesting to discuss the values obtained for the parameters χ_{ij} and x_i that appear in Eqs. (8). For both guar/dextran ratios, the Flory–Huggins parameters, calculated from the second virial coefficients according to Eqs. (10), are $\chi_{12} \sim 0.492$ for dextran/water, $\chi_{13} \sim 0.483$ for guar/water, and $\chi_{23} \sim 0.0037$ for dextran/guar interactions. Water is then a better solvent for guar than for dextran, which could be surprising since dextran can be easily dissolved in water, contrary to guar. However, as discussed on the basis of the phase diagram in a previous paper (Simonet et al., 2000), the dextran-rich phase is more concentrated than the guar-rich one, showing that the affinity between guar and water is greater than between dextran and water (Hsu & Prausnitz, 1974). Moreover, dextran is branched and highly flexible and hence features a more compact structure than guar, which is rather semirigid due to the β-(1 → 4) linkages of the backbone. Therefore, the excluded volume interactions are probably much greater for guar than for dextran, which explains its higher value of second virial coefficient, and consequently, its lower value of polymer–solvent Flory–Huggins parameter according to Eqs. (10a) and (10b). The polymer–polymer interaction parameter χ_{23} is close to zero and slightly positive, which reveals a weak repulsive force between the polymers, high enough to promote phase separation. This result is generally representative of segregative ternary systems in organic solvent (Hsu & Prausnitz, 1974; Zeman & Patterson, 1972) or in aqueous medium (Clark, 2000; Piculell et al., 1995). The parameter

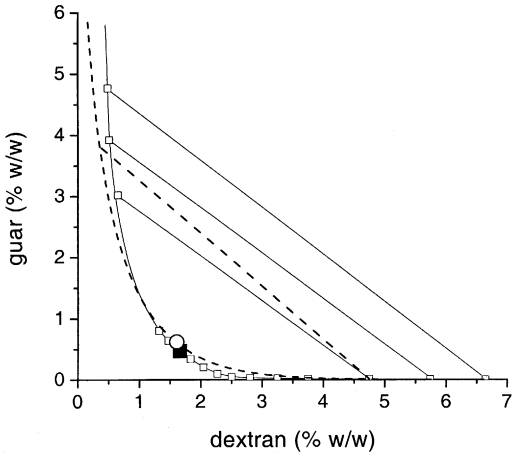

Fig. 6. Calculated binodal and tie-lines for the guar/dextran system using the Flory–Huggins theory and the light scattering data of the 17/83 or the 28/72 mixture (- - -). The experimental binodal and tie-lines are represented with solid lines and symbols (—□—). Open symbol (○) refers to the calculated critical point and (■) represents the experimental critical point.

x_i representing the ratio of polymer i to solvent molar volumes has been calculated for dextran ($x_2 \sim 19,200$) and guar ($x_3 \sim 73,500$) on the basis of weight-average molar weights, the partial specific volume of both polymers ($v_i \sim 0.61\ \mathrm{cm^3\ g^{-1}}$) being determined at 25°C with a pycnometer.

The binodal and tie-lines calculated on the basis of the Flory–Huggins theory are represented for the two guar/dextran ratios in Fig. 6. As previously observed, both ratios yield the same binodal, which is still close to the experimental curve on the whole phase diagram, and more especially at low guar concentration. The slope of the calculated tie-lines is about 0.87 in both cases, which is slightly higher than the experimental value (~0.74). The coordinates of the calculated critical point are about 1.59% w/w dextran and 0.62% w/w guar for both guar/dextran ratios, while the experimental values are 1.66% w/w dextran and 0.47% w/w guar. This slight difference, as well as the small gap between calculated and experimental binodals at low guar concentration, might be explained by the polydispersity of the guar sample (Shirataki & Kamide, 1993), as previously illustrated.

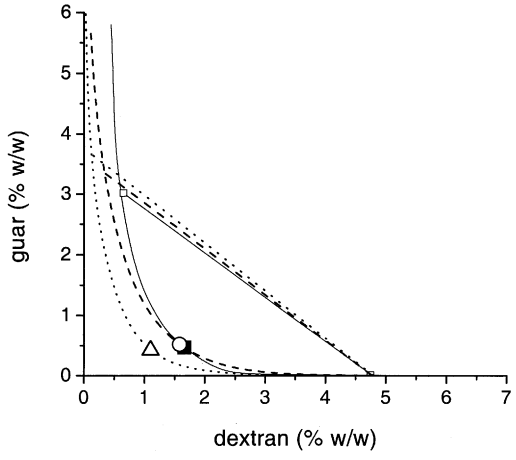

Fig. 7. Calculated binodals and tie-lines for the guar/dextran system using the virial expansion and the light scattering data of the 17/83 mixture. The dotted lines have been calculated by taking the second virial coefficient of guar (A_{33}) equal to $3 \times 10^{-4}\ \mathrm{cm^3\ mol\ g^{-2}}$. These are compared to the results obtained with $A_{33} = 3.25 \times 10^{-4}\ \mathrm{cm^3\ mol\ g^{-2}}$ (dashed lines), as in Fig. 5. Open symbols (△) and (○) refer to the calculated critical points for the two above values, respectively. The experimental binodal and tie-lines (—□—), and critical point (■) are also represented.

It is noteworthy that both thermodynamic approaches lead to very similar calculated phase diagrams. This may be due to the fact that the expressions of chemical potentials detailed in Eqs. (3) and (8) are identical for both models if the polymers volume fractions are low enough, i.e. $\phi_2 \ll 1$ and $\phi_3 \ll 1$, and if the χ_{ij} parameters are replaced by their expressions given in Eqs. (10a)–(10c) in terms of second virial coefficients. Therefore, even though both models display different initial hypothesis and are constructed in a very different way, they may yield identical expressions for the chemical potentials, and hence, similar calculated phase diagrams. Still, the Flory–Huggins theory is limited by some unrealistic hypothesis that do not exist in the virial model (Clark, 2000). For instance, this theory cannot account for branched or semirigid polymers and the entropic term does not take into account the organization of water molecules. Moreover, the χ_{ij} parameters should be considered as free energies that may depend on temperature, concentration, and molar weight.

Another noteworthy feature of both methods is the very high sensitivity to the values of the second virial coefficients. This effect is illustrated in Fig. 7 for the particular case of the virial expansion, on the basis of the 17/83 ratio light scattering data. A lower value is affected to the second virial coefficient of guar, i.e. $A_{33} = 3 \times 10^{-4}\ \mathrm{cm^3\ mol\ g^{-2}}$, corresponding to the lower limit of the interval given by light scattering, instead of $3.25 \times 10^{-4}\ \mathrm{cm^3\ mol\ g^{-2}}$, as used in the previous calculations. This slight change leads to significantly different calculated binodal and critical points that are closer to the guar axis. It is noticeable, however, that the slope of the tie-lines is only slightly affected (0.78 instead of 0.75), indicating that the partition of water is still predicted with a fairly good accuracy. By using higher values for the second virial coefficient of guar, the biphasic area progressively decreases and vanishes for $A_{33} = 4.0 \times 10^{-4}\ \mathrm{cm^3\ mol\ g^{-2}}$, meaning that total miscibility is then predicted. Besides, some trials made with different values of molar weights have shown a relatively low sensitivity to these parameters, suggesting that the use of number-average molar weights would have probably yielded comparable results.

5. Conclusion

A purely predictive approach based exclusively on

experimental measurements was not possible since the second virial coefficient of guar is difficult to obtain by light scattering. Hence, this parameter has been adjusted with a relatively simple criterion leaving the experimental binodal or tie-lines out of consideration. For the guar/dextran ratios 17/83 and 28/72 examined in the present work, this condition led to relatively close values of second virial coefficient for guar, situated within the interval given by light scattering. The calculated phase diagrams for the two ratios were almost superimposed and both thermodynamic approaches, i.e. the virial expansion and the Flory–Huggins theory, yielded relatively similar phase diagrams that satisfactorily described the experimental one. Only slight differences between calculated and experimental binodals and critical points were observed and the slope of the tie-lines was given with a good accuracy, especially with the virial expansion model. Polydispersity of guar and problems due to the extrapolation from the dilute to the semidilute regime might be the major sources of discrepancy. The fact that both approaches yielded analogous results is not surprising, given that the Flory–Huggins parameters were calculated from the second virial coefficients, considering that the polymer concentrations were low enough. In this particular case, both expressions of the chemical potential are indeed equivalent and reflect excluded volume interactions. This global approach has shown that the virial expansion model and the Flory–Huggins theory for "dilute solutions" are adapted to the description of the guar/dextran phase behavior, even though the results obtained in the dilute regime are extrapolated to the semidilute one. However, an outstanding sensitivity to the second virial coefficient values was noticed, indicating that these models can be used to predict experimental results, provided that these parameters are precisely determined. The same approach could be used to describe the partitioning of proteins like bovine serum albumin or β-lactoglobulin in this aqueous two-phase system, on the basis of experimental results obtained in a previous paper (Simonet et al., 2000). The model based on the virial expansion (King et al., 1988), as well as the Flory–Huggins theory (Albertsson et al., 1987; Brooks, Sharp & Fisher, 1985) yielded satisfying results in this matter.

Acknowledgements

Financial support from Rhodia (France) for funding F. Simonet is gratefully acknowledged. Light scattering experiments were performed at the Complex Fluids Laboratory of Rhodia Inc. (Cranbury, New Jersey) under the direction of M. Joanicot, who is particularly acknowledged.

References

Albertsson, P. -Å. (1962). Partition methods for fractionation of cell particles and macromolecules. *Methods of Biochemical Analysis*, *10*, 229–262.

Albertsson, P. -Å. (1986). *Partition of cell particles and macromolecules*, New York: Wiley.

Albertsson, P. -Å., Cajarville, A., Brooks, D.E., & Tjerneld, F. (1987). Partition of proteins in aqueous two-phase systems and the effects of molecular weight on the polymer. *Biochem. Biophys. Acta.*, *926*, 87–93.

Antonov, Y. A., Lefebvre, J., & Doublier, J. -L. (1999). On the one-phase state of aqueous protein–uncharged polymer systems: casein–guar gum system. *Journal of Applied Polymer Science*, *71*, 471–482.

Arond, L. H., & Frank, H. P. (1954). Molecular weight, molecular weight distribution and molecular size of a native dextran. *Journal of Physical Chemistry*, *58*, 953–957.

Brooks, D. E., Sharp, K. A., & Fisher, D. (1985). Theoretical aspects of partitioning. In H. Walter, D. E. Brooks & D. Fisher, *Partitioning in aqueous two-phase systems: theory, methods, uses, and applications to biotechnology* (pp. 11–84). London: Academic Press.

Burchard, W., & Pfannemüller, B. (1969). Molekulargewichte von Dextran und Dextrantricarbanilat des Bakterienstammes Leuconostoc Mesenteroides B 512. *Die Makromolekulare Chemie*, *121*, 18–32.

Cabezas Jr., H., Evans, J. D., & Szlag, D. C. (1989). A statistical mechanical model of aqueous two-phase systems. *Fluid Phase Equilibria*, *53*, 453–462.

Clark, A. H. (2000). Direct analysis of experimental tie line data (two polymer–one solvent systems) using Flory–Huggins theory. *Carbohydrate Polymers*, *42*, 337–351.

Closs, C. B., Conde-Petit, B., Roberts, I. D., Tolstoguzov, V. B., & Escher, F. (1999). Phase separation and rheology of aqueous starch/galactomannan systems. *Carbohydrate Polymers*, *39*, 67–77.

Desbrières, J., Borsali, R., Rinaudo, M., & Milas, M. (1993). (X_F interaction parameter and single-chain diffusion coefficients of dextran/poly(vinylpyrrolidone)/water: dynamic light scattering experiments. *Macromolecules*, *26*, 2592–2596.

Doublier, J. -L. (1975). *Propriétés rhéologiques et caractéristiques macromoléculaires de solutions aqueuses de galactomannanes*. PhD thesis, Université Paris 6.

Doublier, J. -L., & Launay, B. (1981). Rheology of galactomannan solutions: comparative study of guar gum and locust bean gum. *Journal of Texture Studies*, *12*, 151–172.

Edmond, E., & Ogston, A. G. (1968). An approach to the study of phase separation in ternary aqueous systems. *Biochemistry Journal*, *109*, 569–576.

Flory, P. J. (1942). Thermodynamics of high polymer solutions. *Journal of Chemical Physics*, *10*, 51–61.

Flory, P. J. (1953). *Principles of polymer chemistry*, Ithaca, NY: Cornell University Press.

Garnier, C., Schorsch, C., & Doublier, J. -L. (1995). Phase separation in dextran/locust bean gum mixtures. *Carbohydrate Polymers*, *28*, 313–317.

Garnier, C., Bouchet, B., Gallant, D. -J., & Doublier, J. -L. (1999). Ultrastructure et comportement rhéologique de mélanges de biopolymères à base de galactomannanes. *Sciences des Aliments*, *19*, 459–470.

Großmann, C., Tintinger, R., Zhu, J., & Maurer, G. (1995). Aqueous two-phase systems of poly(ethylene glycol) and dextran — experimental results and modelling of thermodynamic properties. *Fluid Phase Equilibria*, *106*, 111–138.

Guan, Y., Lilley, T. H., & Treffry, T. E. (1993). A new excluded volume theory and its application to the coexistence curves of aqueous polymer two-phase systems. *Macromolecules*, *26*, 3971–3979.

Haynes, C. A., Beynon, R. A., King, R. S., Blanch, H. W., & Prausnitz, J. M. (1989). Thermodynamic properties of aqueous polymer solutions: poly(ethylene glycol)/dextran. *Journal of Physical Chemistry*, *93*, 5612–5617.

Haynes, C. A., Benitez, F. J., Blanch, H. W., & Prausnitz, J. M. (1993). Application of integral-equation theory to aqueous two-phase partitioning systems. *AIChE Journal*, *39*, 1539–1557.

Hsu, C. C., & Prausnitz, J. M. (1974). Thermodynamics of polymer compatibility in ternary systems. *Macromolecules*, *7*, 320–324.

Huggins, M. L. (1942). Theory of solutions of high polymers. *Journal of the American Chemical Society*, *64*, 1712–1719.

Kalichevsky, M. T., & Ring, S. G. (1987). Incompatibility of amylose and amylopectin in aqueous solution. *Carbohydrate Research*, *162*, 323–328.

Kalichevsky, M. T., Orford, P. D., & Ring, S. G. (1986). The incompatibility of concentrated aqueous solutions of dextran and amylose and its effect on amylose gelation. *Carbohydrate Polymers*, *6*, 145–154.

Kang, C. H., & Sandler, S. I. (1987). Phase behavior of aqueous two-polymer systems. *Fluid Phase Equilibria*, *38*, 245–272.

Kang, C. H., & Sandler, S. I. (1988). Effects of polydispersivity on the phase behavior of aqueous two-phase polymer systems. *Macromolecules*, *21*, 3088–3095.

King, R. S., Blanch, H. W., & Prausnitz, J. M. (1988). Molecular thermodynamics of aqueous two-phase systems for bioseparations. *AIChE Journal*, *34*, 1585–1594.

Koningsveld, R., & Staverman, A. J. (1968). Liquid–liquid phase separation in multicomponent polymer solutions. II. The critical state. *Journal of Polymer Science A-2*, *6*, 325–348.

Kratochvíl, P. (1972). Particle scattering functions. In M. B. Huglin, *Light scattering from polymer solutions* (pp. 333–384). New York: Academic Press.

Kratochvíl, P., Vorlícek, J., Straková, D., & Tuzar, Z. (1975). Light scattering investigation of interaction between polymers in dilute solution. *Journal of Polymer Science: Polymer Physics Edition*, *13*, 2321–2329.

McDougall, A. J., Rigby, N. M., & Ring, S. G. (1997). Phase separation of plant cell wall polysaccharides and its implications for cell wall assembly. *Plant Physiology*, *114*, 353–362.

Medin, A. S., & Janson, J. -C. (1993). Studies on aqueous polymer two-phase systems containing agarose. *Carbohydrate Polymers*, *22*, 127–136.

Mumby, S. J., & Sher, P. (1994). Determination of χ from liquid–liquid phase data and the computation of phase diagrams for quasi-binary polymer solutions and blends. *Macromolecules*, *27*, 689–694.

Piculell, L., Bergfeldt, K., & Nilsson, S. (1995). Factors determining phase behaviour of multi component polymer systems. In S. E. Harding, S. E. Hill & J. R. Mitchell, *Biopolymer mixtures* (pp. 13–35). Nottingham: Nottingham University Press.

Prigogine, I., & Defay, R. (1954). *Chemical thermodynamics*, London: Longmans, Green and Co (chap 16, pp. 225–250).

Rathbone, S. J., Haynes, C. A., Blanch, H. W., & Prausnitz, J. M. (1990). Thermodynamic properties of dilute aqueous polymer solutions from low-angle laser light scattering measurements. *Macromolecules*, *23*, 3944–3947.

Robinson, G., Ross-Murphy, S. B., & Morris, E. R. (1982). Viscosity–molecular weight relationships, intrinsic chain flexibility and dynamic solution properties of guar galactomannan. *Carbohydrate Research*, *107*, 17–32.

Sabater de Sabates, A. (1979). *Contribution à l'étude des relations entre caractéristiques macromoléculaires et propriétés rhéologiques en solution aqueuse concentrée d'un épaississant alimentaire: la gomme de caroube*. PhD thesis, Université Paris 11.

Scott, R. L. (1949). The thermodynamics of high polymer solutions. V. Phase equilibria in the ternary system: polymer 1–polymer 2–solvent. *Journal of Chemical Physics*, *17*, 279–284.

Senti, F. R., Hellman, N. N., Ludwig, N. H., Babcock, G. E., Tobin, R., Glass, C. A., & Lamberts, B. L. (1955). Viscosity, sedimentation, and light-scattering properties of fractions of an acid-hydrolyzed dextran. *Journal of Polymer Science*, *17*, 527–546.

Shirataki, H., & Kamide, K. (1993). Phase equilibria of quasi-ternary systems consisting of multicomponent polymers 1 and 2 in a single solvent. II. Cloud point curve. *Polymer International*, *32*, 265–273.

da Silva, L. H. M., & Meirelles, A. J. A. (2000). Phase equilibrium in polyethylene glycol/maltodextrin aqueous two-phase systems. *Carbohydrate Polymers*, *42*, 273–278.

Simonet, F., Garnier, C., & Doublier, J. -L. (2000). Partition of proteins in the aqueous guar/dextran two-phase system. *Food Hydrocolloids*, *14*, 591–600.

Tolstoguzov, V. B. (1998). Functional properties of protein–polysaccharide mixtures. In S. E. Hill, D. A. Ledward & J. R. Mitchell, *Functional properties of food macromolecules* (pp. 252–277). Gaithersburg, Maryland: Aspen Publishers.

Tompa, H. (1949). Phase relationships in polymer solutions. *Transactions of the Faraday Society*, *45*, 1142–1152.

Tvaroska, I., Perez, S., & Marchessault, R. H. (1978). Conformational analysis of (1–6)-α-D-glucan. *Carbohydrate Research*, *61*, 97–106.

Vinches, C., Parker, A., & Reed, W. F. (1997). Phase behavior of aqueous gelatin/oligosaccharide mixtures. *Biopolymers*, *41*, 607–622.

Wu, C. (1993). Laser light-scattering characterisation of the molecular weight distribution of dextran. *Macromolecules*, *26*, 3821–3825.

Wu, Y. -T., Zhu, Z. -Q., Lin, D. -Q., & Mei, L. -H. (1996). A modified NRTL equation for the calculation of phase equilibrium of polymer solutions. *Fluid Phase Equilibria*, *121*, 125–139.

Zaslavsky, B. Yu. (1995). *Aqueous two-phase partitioning*, *Physical chemistry and bioanalytical applications*. New York: Marcel Dekker.

Zeman, L., & Patterson, D. (1972). Effect of the solvent on polymer incompatibility in solution. *Macromolecules*, *5*, 513–516.